

# An x-ray fluorescence holographic study on a $\text{Bi}_2\text{Te}_3\text{Mn}_{0.1}$ topological insulator

S Hosokawa<sup>1</sup>, N Happo<sup>2</sup>, K Hayashi<sup>3</sup>, A Ohnishi<sup>4</sup>, M Kitaura<sup>4</sup> and M Sasaki<sup>4</sup>

<sup>1</sup>Department of Physics, Graduate School of Science and Technology, Kumamoto University, Kumamoto 860-8555, Japan

<sup>2</sup>Graduate School of Information Sciences, Hiroshima City University, Hiroshima 731-3194, Japan

<sup>3</sup>Institute of Materials Research, Tohoku University, Sendai 980-8577, Japan

<sup>4</sup>Department of Physics, Faculty of Science, Yamagata University, Yamagata 990-8560, Japan

E-mail: hosokawa@sci.kumamoto-u.ac.jp

**Abstract.** To search the atomic sites of Mn impurities in  $\text{Bi}_2\text{Te}_3\text{Mn}_{0.1}$  topological insulator, a Mn  $K\alpha$  fluorescence x-ray holography experiment was performed. The reconstructed atomic image around the central Mn atom reveals a hexagonal configuration, where the local lattice constant is slightly larger than the original  $\text{Bi}_2\text{Te}_3$  crystal. Thus, the most plausible atomic position of Mn impurities is the substitution with Bi or Te atom. The further-distant atomic images are hardly observed unlike usual crystals, indicating a formation of flat clusters around Mn in this functional crystal.

## 1. Introduction

In the past,  $\text{Bi}_2\text{Te}_3$  was well-known as a thermoelectric material having a large value of thermopower. Nowadays, this material has also achieved much attention as a topological insulator, where the so-called Dirac electrons with an almost zero mass can conduct on the surface of this material. From this reason,  $\text{Bi}_2\text{Te}_3$  is promising as a raw material for future computer systems of very fast and energy-saving.

$\text{Bi}_2\text{Te}_3$  is essentially a  $p$ -type degenerate semiconductor (SC). By adding electrons, e.g., increasing Te concentration, it becomes a topological insulator (TI), and then  $n$ -type degenerate SC. However, the TI properties in  $\text{Bi}_2\text{Te}_{3+\delta}$  has a very short lifetime due to surface contaminations, and thus, this material is not suitable for the applicational use.

Recently, Sasaki and coworkers [1] found that Mn- and some other impurity(M)-doped  $\text{Bi}_2\text{Te}_3\text{M}_x$  alloys have a similar behavior. Up to  $x = 0.05$ , it shows  $p$ -type SC, and beyond  $x = 0.075$  it becomes  $n$ -type SC. The TI phase is located between  $x = 0.05$  and  $0.075$ . Moreover, they found some interesting features as TI materials. Firstly, the lifetime of the TI properties is extremely long, which is very important for applications. Secondly, the Dirac electrons are not scattered by impurities (clean surface Dirac electrons), which was detected by a magnetoresistance measurement at low temperature.

Then, an important question arises: Where do the impurity atoms locate in the  $\text{Bi}_2\text{Te}_3$  crystal for showing such excellent TI properties?  $\text{Bi}_2\text{Te}_3$  has a layer structure with a hexagonal form [2]. Figure 1 shows one layer of the  $\text{Bi}_2\text{Te}_3$  crystal. There are two types of Te atoms in the layer.



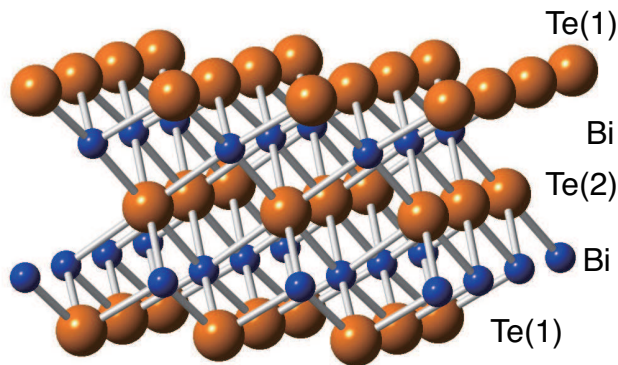


**Figure 1.** (Color online.) One layer in the  $\text{Bi}_2\text{Te}_3$  hexagonal crystal [2]. Large and small balls indicate Te and Bi atoms, respectively.

One is on the surface of layers, Te(1), where a van der Waals force combines the layers, and another is at the center of layers, Te(2), which connects with Bi atoms by a covalent-ionic mixed binding. The interlayer positions would be most plausible for the impurities, but there is no reason to exclude the possibilities of substitutions with Bi or Te atoms or interstitial positions in the layer.

X-ray fluorescence holography (XFH) is a newly developed technique that enables one to draw three-dimensional (3D) atomic images around a specific element emitting fluorescent x-rays [3]. Due to the interference between the direct incident x-rays and those scattered by the surrounding atoms, the fluorescent x-ray intensity from the emitter slightly modulates with the incident x-ray angles by about 0.1%, from which 3D images can be obtained by simple Fourier transforms without any special models. We have performed the Mn  $K\alpha$  XFH measurements on  $\text{Bi}_2\text{Te}_3\text{Mn}_{0.1}$  single crystal at room temperature. In this paper, we report atomic images around the Mn atoms.

## 2. Experimental procedure and data analysis

A single crystal of  $\text{Bi}_2\text{Te}_3\text{Mn}_{0.1}$  was grown by a modified Bridgman method, where  $\text{Bi}_2\text{Te}_3$  and Mn powders were melted and crystallized in an evacuated quartz ampoule several times by slow cooling. The sample was cooled from  $850^\circ\text{C}$  to  $550^\circ\text{C}$  with a cooling rate of  $10^\circ\text{C}/\text{h}$ . The crystal was cut and polished so as to have a (001) flat surface larger than  $5 \times 5 \text{ mm}^2$ . The crystallinity of the sample was examined by taking a Laue photograph.

XFH measurements were carried out at the beamlines BL6C in the Photon Factory at the High Energy Accelerator Research Organization (PF-KEK), in Tsukuba, Japan. The sample was placed on a two-axes table of a diffractometer. The measurements were performed in inverse mode by rotating the two axes, the exit angle of  $0^\circ \leq \theta \leq 75^\circ$  in steps of  $1.00^\circ$ , and the azimuthal angle of  $0^\circ \leq \phi \leq 360^\circ$  in steps of about  $0.35^\circ$ , of the sample stage. Incident x-rays were focused onto the (001) surface of the samples. Mn  $K\alpha$  fluorescent x-rays were collected using an avalanche photodiode detector with a cylindrical graphite crystal energy-analyzer. The XFH signals were recorded at eight different incident x-ray energies from 7.0 to 10.5 keV in steps of 0.5 keV. Each scan took about 12 h. Details of the experimental setup are given elsewhere [3].

Holographic oscillation data were obtained by subtracting the background from the fluorescent x-ray intensities and normalizing them to the incident x-ray intensities. An extension of the hologram data was carried out using the crystal symmetry of the hexagonal structure [2] and the measured x-ray standing wave (XSW) lines. From the hologram patterns, 3D atomic configuration images were reconstructed using Barton's algorithm [4] by superimposing the holograms with eight different incident x-ray energies, which can highly suppress the appearance of twin images.

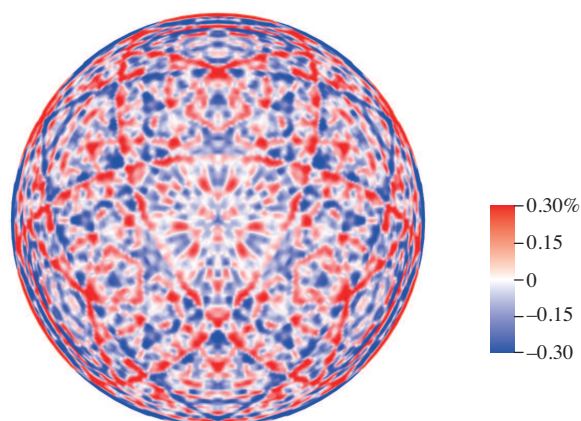


**Figure 2.** (Color online.) Examples of Mn  $K\alpha$  hologram pattern obtained from (001) surfaces of  $\text{Bi}_2\text{Te}_3\text{Mn}_{0.1}$  single crystal measured at incident x-ray energy of 8.0 keV.

### 3. Results and discussion

Figure 2 shows examples of the Mn  $K\alpha$  hologram pattern of the  $\text{Bi}_2\text{Te}_3\text{Mn}_{0.1}$  single crystal measured at an incident x-ray energy of 8.0 keV. The radial and angle directions indicate  $\theta$  and  $\phi$ , respectively, and the magnitudes are given as the color bars beside the figure. A roughly threefold symmetry including XSW signals was observed in the holographic pattern, indicating a good quality of the sample crystal.

Figure 3 shows the reconstructed atomic image of  $\text{Bi}_2\text{Te}_3\text{Mn}_{0.1}$  single crystal on the (001) plane around the central Mn atom marked by the circle in the figure. The image intensities were normalized to that of the strongest atoms, and are shown as the color bar beside the figure. To avoid confusions on the noise level artifacts and to emphasize the middle intensity range, the color variation was chosen to range from 0.25 to 0.75. As a guide for eyes, cross-sections of dashed lines indicate ideal positions of the neighboring atoms obtained from x-ray diffraction (XD) [2] provided that the Mn atom is located at a Bi or Te position. As seen in Fig. 1, all of atoms on the (001) plane are the same element, Bi or Te, depending on the  $z$  value along the  $c$  axis.

As seen in Fig. 3, clear six atomic images are observed near the ideal positions of the hexagonal lattice. Thus, the Mn impurity atom does not enter an interlayer position, and would

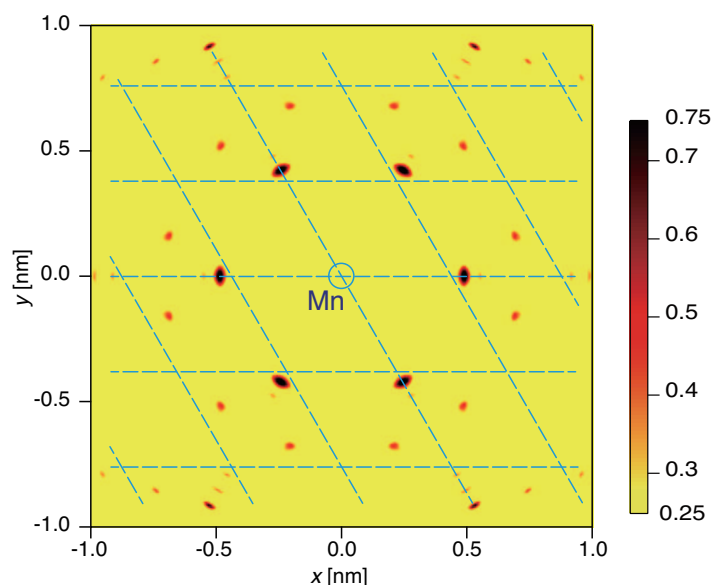


**Figure 3.** (Color online.) Atomic images of  $\text{Bi}_2\text{Te}_3\text{Mn}_{0.1}$  single crystal on (001) plane around central Mn atoms marked by the circle. Cross-sections of dashed lines indicate ideal positions of neighboring atoms obtained from XD [2] provided that the Mn atom is located at a Bi or Te position.

be located at a substitutional position of Bi or Te atoms in the original  $\text{Bi}_2\text{Te}_3$  crystal. Since the nearest-neighboring atoms are hardly visible (not shown in the figure) unlike usual covalent crystals, such as ZnTe [5] or GaSb [6], the Mn impurity atom would locate at a flexible site, and thus, it is most plausible that the Mn impurity atoms are substituted with an interlayer Te atom, Te(1) in Fig. 1. However, there is no reason to exclude the possibilities of substitutions with Bi or Te(2) atoms inside the layer.

Recently, an XAFS study was carried out on  $(\text{Bi}_{1-x}\text{Mn}_x)_2\text{Te}_3$  epitaxial thin film crystal of impurity substitutional type, and it was concluded that the Mn impurities are located at the interlayer positions [7]. However, such positions of Mn impurity do not make the hexagonal lattice of Bi or Te atoms on the (001) plane around the central Mn atom.

The local lattice constant around the Mn impurity is slightly larger than the original  $\text{Bi}_2\text{Te}_3$  crystal. Note that the present XFH shows only images of the second neighboring Te atoms, and the other images are hardly visible (not shown). As discussed in a previous paper on mixed crystals [5, 6, 8], an impurity induces strong fluctuations in nearest-neighboring atomic positions, which results in very weak atomic images of nearest-neighboring atoms. In this material, however, further distant neighboring atoms are not observed unlike previous mixed crystals. From these findings, it would be reasonable to conclude that a strong flat clusters are formed, and the positional fluctuations between the clusters are very large.

#### 4. Conclusion

We have carried out a Mn  $K\alpha$  fluorescence x-ray holography experiment on  $\text{Bi}_2\text{Te}_3\text{Mn}_{0.1}$  topological insulator. The reconstructed atomic image around the central Mn atom reveals a hexagonal configuration, where the local lattice constant is slightly larger than the original  $\text{Bi}_2\text{Te}_3$  crystal. The plausible atomic position of Mn impurities is the substitution with Bi or Te atom. The further-distant atomic images are hardly observed unlike usual crystals, indicating a formation of flat clusters around Mn in this functional crystal. To confirm these results, a Bi  $L\alpha$  XFH experiment and a more detailed XAFS measurement are essential, which are now in progress.

#### Acknowledgments

The authors thank Professor S. Sasaki of Tokyo Institute of Technology for the support of the XFH experiments. NH and KH acknowledge the Japan Society for the Promotion of Science (JSPS) for Grants-in-Aid for Scientific Research (Nos. 24560016 and 22360264). This work was performed under the inter-university cooperative research program of Institute for Materials Research, Tohoku University (Project Nos. 11K0008 and 12K0034). The XFH experiments were performed at BL6C of PF-KEK (Proposal No. 2011G530).

#### References

- [1] Kim H-J, Kim K-S, Kim M D, Lee S-J, Han J-W, Ohnishi A, Kitaura M, Sasaki M, Kondo A and Kindo K 2011 *Phys. Rev. B* **84** 125144
- [2] Feutelais Y, Legendre B, Rodier N and Agafonov V 1993 *Mater. Res. Bull.* **28** 591
- [3] Hayashi K, Happo N, Hosokawa S, Hu W and Matsushita T 2012 *J. Phys.: Condens. Matter* **24** 093201
- [4] Barton J J 1991 *Phys. Rev. Lett.* **67** 3106
- [5] Hosokawa S, Happo N and Hayashi K 2009 *Phys. Rev. B* **80** 134123
- [6] Hosokawa S, Happo N, Ozaki T, Ikemoto H, Shishido T and Hayashi K 2013 *Phys. Rev. B* **87** 094104
- [7] Strohm C, Bauer G, Holy V, Springholz G, Caha O, Ruzicka J and Steiner H 2013 *ESRF Report* HE-3932
- [8] Happo N, Hayashi K and Hosokawa S 2009 *J. Cryst. Growth* **311** 990